



## The gamma-matrix concept, a method for treating heterogeneities in diffusion calculations

Petersen, T.; Kirkegaard, Peter

*Publication date:*  
1973

*Document Version*  
Publisher's PDF, also known as Version of record

[Link back to DTU Orbit](#)

*Citation (APA):*  
Petersen, T., & Kirkegaard, P. (1973). *The gamma-matrix concept, a method for treating heterogeneities in diffusion calculations*. Risø National Laboratory. Risø-M No. 1607

---

### General rights

Copyright and moral rights for the publications made accessible in the public portal are retained by the authors and/or other copyright owners and it is a condition of accessing publications that users recognise and abide by the legal requirements associated with these rights.

- Users may download and print one copy of any publication from the public portal for the purpose of private study or research.
- You may not further distribute the material or use it for any profit-making activity or commercial gain
- You may freely distribute the URL identifying the publication in the public portal

If you believe that this document breaches copyright please contact us providing details, and we will remove access to the work immediately and investigate your claim.

1607

Risø - M -

<p>Title and author(s)</p> <p>The <math>\gamma</math>-Matrix Concept, a Method for Treating Heterogeneities in Diffusion Calculations</p> <p>by</p> <p>Torben Petersen and Peter Kirkegaard</p>	<p>Date</p> <hr/> <p>Department or group</p> <p>Reactor Physics Department</p> <hr/> <p>Group's own registration number(s)</p>
<p>pages + 4    tables + 7    illustrations</p>	
<p><b>Abstract</b></p> <p>A method for treating heterogeneities in diffusion calculations for a reactor is described. It is done by means of the <math>\gamma</math>-matrix concept. The heterogeneity is treated as a black box, and the <math>\gamma</math>-matrix provides the coupling between the diffusion calculation and the black box.</p> <p>A Monte Carlo code, MOVAX, for calculating the <math>\gamma</math>-matrix for a cruciform BWR control rod is described.</p>	<p><b>Copies to</b></p> <p>Standard distribution    125 copies</p> <hr/> <p><b>Abstract to</b></p>
<p>Available on request from the Library of the Danish Atomic Energy Commission (Atomenergi-kommissionens Bibliotek), Risø, Roskilde, Denmark. Telephone: (03) 35 51 01, ext. 334, telex: 5072.</p>	

CONTENTS

	Page
1. The $\gamma$ -Matrix Concept .....	2
1.1. Introduction and Definition .....	2
1.2. Foundations for Calculation of a $\gamma$ -Matrix ..	3
1.3. A Collision Probability Method for Calculating a $\gamma$ -Matrix .....	4
2. Monte Carlo Calculation of the $\gamma$ -Matrix .....	5
2.1. Representation of Cruciform Control Rods in BWR's .....	5
2.2. Principles of the Monte Carlo Calculation ...	5
2.3. The Monte Carlo Program MOVAX .....	8
2.3.1. Data Input .....	8
2.3.2. Sorting .....	8
2.3.3. Direct Simulation Block .....	8
2.3.4. Estimates of <u>A</u> and <u>B</u> .....	9
2.3.5. $\gamma$ -Estimate by Matrix Inversion .....	9
2.3.6. Statistical Processing .....	9
2.3.7. Output .....	9
3. Test of the MOVAX Program .....	10
3.1. Comparisons with other Methods .....	10
3.2. Test of Statistical Stability .....	11
4. Conclusion .....	12
References .....	13
Tables .....	14
Figures .....	18

## 1. THE $\gamma$ -MATRIX CONCEPT

### 1.1. Introduction and Definition

The flux distribution in power reactors can normally be found by application of diffusion theory, provided strong heterogeneities, such as control rods, are separately taken care of by other methods. The basic idea of such an approach is to use some sort of transport theory in a limited area containing the heterogeneity and afterwards include the effect of this in the diffusion calculation. A normal homogenisation is one example of such a method. Another is to consider the heterogeneity as external to the diffusion medium, and represent the boundary between this and the heterogeneity by some boundary condition. In both cases the aim is to find a representation of the heterogeneity, which responds correctly to conditions in the diffusion medium, independently of these. This leads to a formulation in terms of the black-box concept.

In a single-group diffusion calculation an adequate representation is the usual boundary condition

$$J = \alpha \phi \quad (1)$$

relating the net current  $J$  to the surface flux  $\phi$  by the coefficient  $\alpha = \frac{D}{\lambda}$ , where  $D$  is the diffusion coefficient and  $\lambda$  the extrapolation length. In a multi-group scheme without up- and downscattering in the heterogeneity, (1) should be replaced by a matrix equation

$$\underline{J} = \underline{\alpha} \underline{\phi} \quad (2)$$

$\underline{J}$  and  $\underline{\phi}$  are now vectors containing the  $G$ -group currents and fluxes, and  $\underline{\alpha}$  is a  $G \times G$  diagonal matrix with the elements

$$\alpha_{gg} = \frac{D_g}{\lambda_g} \quad (3)$$

in perfect analogy to the one-group case. If the heterogeneity contains up- and downscattering material, we may still postulate

a linear relationship between group currents and fluxes at the surface:

$$\underline{J} = \underline{\gamma} \cdot \underline{\phi} \quad (4)$$

but the matrix  $\underline{\gamma}$  will in this case contain off-diagonal elements, since a neutron entering group  $g$  can return in group  $g' \neq g$ . The GxG matrix  $\underline{\gamma}$  will be called the  $\gamma$ -matrix for the heterogeneity. If we take as sign conventions that the current is positive out of the diffusion medium, then  $\gamma_{gg} > 0$  for  $g=g'$  and  $\gamma_{gg} < 0$  for  $g \neq g'$ .

It should be emphasized that (4) is only valid when  $\underline{J}$  and  $\underline{\phi}$  are calculated by diffusion theory. In the physical situation only that part of the neutrons that actually crosses the boundary will contribute to the currents, while  $\phi$  is the isotropic flux component and thus also contains neutrons moving away from the boundary. Implications of this will be mentioned in the following section.

### 1.2. Foundations for Calculation of a $\gamma$ -Matrix

The basis of the calculation of the  $\gamma$ -matrix is a matching at the boundary of a transport calculation in the heterogeneity to a diffusion calculation in the surrounding medium.

Diffusion theory only involves the two first terms in the Legendre expansion of the angular flux. In slab geometry, for example the angular flux in group  $g$  is

$$\phi^g(\mu, z) = \frac{1}{2} \phi_0^g(z) + \frac{3}{2} \phi_1^g(z) \mu \quad (5)$$

where the symbols are defined in fig. 1.

It will only be possible to require continuity of the isotropic flux  $\phi_0^g$  and the current  $\phi_1^g$ , i.e. continuity of

$$\int_{-1}^1 \phi^g(\mu, z) d\mu \quad \text{and} \quad \int_{-1}^1 \phi^g(\mu, z) \mu d\mu \quad (6)$$

This implies that the boundary should be placed in an area where diffusion theory is valid, i.e. when a  $\gamma$ -matrix is used to represent a cruciform control rod, the boundary should be placed in

the water gap between the rod surface and the fuel element in such a distance from the rod that the flux gradient is small at the boundary. This also overcomes the problem that (4) is only valid for diffusion theory.

### 1.3. A Collision Probability Method for Calculating a $\gamma$ -Matrix

In order to clarify the approximations involved when a  $\gamma$ -matrix is used, a collision probability method for calculating the  $\gamma$ -matrix for a symmetric slab is summarized. The method is described in ref. 1. The geometry is shown in fig. 1.

At first the conservation equations for the slab are set up. As boundary conditions for these equations are used the outgoing currents  $J_g^{\text{out}}$  and the ingoing currents  $J_g^{\text{in}}$ . Considering the right surface of the heterogeneity in fig. 1, these are

$$\begin{aligned} J_{\text{in}}^g &= - \int_{-1}^0 \phi^g(z, \mu) \mu d\mu \\ J_{\text{out}}^g &= \int_0^1 \phi^g(z, \mu) \mu d\mu \end{aligned} \quad (7)$$

From (7), the net current, group  $g$ , into the slab is

$$J^g = J_{\text{in}}^g - J_{\text{out}}^g \quad (8)$$

Since diffusion theory should be valid at the surface, the surface flux is

$$\phi_s^g = 2(J_{\text{in}}^g + J_{\text{out}}^g) \quad (9)$$

The boundary conditions for the conservation equations are then transformed from  $J_{\text{in}}^g$  and  $J_{\text{out}}^g$  to  $J^g$  and  $\phi_s^g$  by means of (8) and (9).  $J^g$  can now be eliminated and  $\phi_s^g$  used as sole boundary condition for the flux in the slab.

The surface flux is then set to

$$\phi_s^g = \delta_{gg'} \quad (10)$$

where  $\delta_{gg'}$  is the Kronecker delta, and the flux distribution in the slab is found. Using the flux distribution,  $J^g$  can be found,

and we have

$$\gamma_{gg'} = J^g \quad \text{where} \quad g = 1, 2, \dots, G \quad (11)$$

and  $G$  is the number of groups.

The calculation is carried out for  $g' = 1, 2, \dots, g$  and thus the whole  $\gamma$ -matrix is found.

## 2. MONTE CARLO CALCULATION OF THE $\gamma$ -MATRIX

### 2.1. Representation of Cruciform Control Rods in BWR's

An obvious problem to solve by means of  $\gamma$ -matrices is the representation of cruciform control rods in boiling water reactors. Although the boundary condition for the surface of the rod probably will vary from the tip of the control blade to the intersection of the blades, a  $\gamma$ -matrix calculated for a slab having the same cross section as the control blade will yield satisfactory results. This has been demonstrated in refs. 2 and 5.

The ordinary design of a BWR control rod makes the calculation of the  $\gamma$ -matrix more complicated than that for a simple slab. A typical cross section of a control blade is shown in fig. 2.

Again it would be possible to use a collision probability method. However, it has been chosen to use a Monte Carlo method in this case.

### 2.2. Principles of the Monte Carlo Calculation

In the following sections it will be described how the Monte Carlo calculation is set up.

We consider a configuration which is symmetrical relative to a central plane. The heterogeneity is region II and the surrounding medium is region I. The fine-structure of region II was depicted in fig. 2. However, the present method would work equally well on any other symmetrical heterogeneity as well as in other one-dimensional geometries (spherical and infinitely cylindrical).

According to the black-box principle, region II is disconnected from I during calculation of the boundary conditions; hence all Monte Carlo histories are confined to region II. The idea is that we realize G different physical situations by Monte Carlo simulation, with one realization mode for each energy group  $g$  ( $g = 1, \dots, G$ ). In mode no  $g$ ,  $N$  neutrons are started in energy group  $g$  with an inward cosine distribution from the boundary (region II is internal in this context). The starter represents an ingoing group current vector

$$J_{I \rightarrow II} = \delta_{gg'} \quad (12)$$

and an ingoing group flux vector

$$\phi_{I \rightarrow II} = 2\delta_{gg'} \quad (13)$$

( $g' = 1, \dots, G$ ).

For each starter a trajectory (fig. 3) is constructed by a direct simulation procedure discussed later. Trajectory no  $i$  ( $i = 1, \dots, N$ ) may terminate by an absorption in II, in which case we assign to it the return weight  $w_i = 0$ . Alternatively, the particle may return to the boundary in some energy group  $g_i$  and with some final direction  $\theta_i$  relative to the normal of the surface; in this case we define  $w_i = 1$ . Now

$$\frac{1}{N} \sum_{i=1}^N w_i \delta_{g_i g'} \quad (14) \quad \text{and} \quad \frac{1}{N} \sum_{i=1}^N w_i \delta_{g_i g'} \frac{1}{\cos \theta_i} \quad (15) \quad (g' = 1, \dots, G)$$

will clearly form unbiased estimators of the outgoing current and flux vectors, resp.; consequently

$$J_i^g = \delta_{gg'} - \frac{1}{N} \sum_{i=1}^N w_i \delta_{g_i g'} \quad (16)$$

and

$$\phi_i^g = 2\delta_{gg'} + \frac{1}{N} \sum_{i=1}^N w_i \delta_{g_i g'} \frac{1}{\cos \theta_i} \quad (17)$$

( $g' = 1, \dots, G$ )



form unbiased estimators of the net-current vector and the total-flux vector for mode  $g$ . When all  $G$  modes are completed, we have sampled  $G$  net-current and  $G$  flux vectors. These can be arranged in  $G \times G$  matrices,  $\underline{A}$  and  $\underline{B}$ , which are non-singular because the modes are linearly independent. Hence, a matrix  $\underline{Y}$  exists which satisfies the equation

$$\underline{A} = \underline{Y} \cdot \underline{B} \tag{18}$$

The whole Monte Carlo procedure sketched above is repeated to get new statistical estimates of  $\underline{Y}$ ; after  $K$  cycles we finally calculate an average  $\gamma$ -matrix

$$\langle \underline{Y} \rangle = \frac{1}{K} \sum_{k=1}^K \underline{Y}_k \tag{19}$$

and a corresponding matrix  $\underline{s}$  of standard deviations from the observed sample variances of the elements.  $\langle \underline{Y} \rangle$  itself is a nearly unbiased estimator of the  $\gamma$ -matrix discussed earlier.

The statistical analysis is complicated by the fact that the applied flux estimator contains the factor  $\frac{1}{\cos\theta_i}$ . If the outgoing flux is halfisotropic, this will induce infinite variance into the elements of  $\underline{B}$ . The Monte Carlo procedure to obtain  $\underline{B}$  is still convergent, but large and irregular fluctuations may occur. The theoretical distribution of  $\underline{Y} = \underline{A} \underline{B}^{-1}$  is very difficult to predict, but in contrast to  $\underline{B}$  it is expected that the elements of  $\underline{B}^{-1}$  have finite population variances; the same will be true for  $\underline{Y}$  and  $\langle \underline{Y} \rangle$ . Thus we expect that our procedure to calculate  $\underline{Y}$  is statistically stable: if  $N$  is large, the distribution of  $\underline{Y}$  is multi-normal, and if  $K$  is not too small,  $\underline{s}$  is a valid estimate of the standard-deviation matrix for  $\langle \underline{Y} \rangle$ .

To estimate the overall statistical quality of the method, it is insufficient to consider the behaviour of  $\langle \underline{Y} \rangle$  (and  $\underline{s}$ ). As  $\underline{Y}$  is only a boundary condition to a subsequent diffusion calculation, it is more relevant to study directly the statistical behaviour of physical output quantities from the latter, like  $k_{eff}$ . We shall return to this point in sec. 3.2.

### 2.3. The Monte Carlo Program MOVAX

A Fortran program MOVAX (AEK P-685) was written along the lines sketched above. Below is given a short description of the elements of the corresponding flow diagram (fig. 4).

#### 2.3.1. Data Input

The following input data are read from punched cards: Number of groups  $G$ , number of regions  $R$ , geometrical data; absorption cross-sections and scattering matrices in all regions with allowance for repetitions; Monte Carlo data (sample blocksize  $N$ , allocated CPU-time, initial pseudo-random integer).

#### 2.3.2. Sorting

The transition between groups is a Markovian process governed by the scattering matrix in the different regions. From this a probability matrix  $P$  is calculated by normalization. We want to minimize the number of invoked random numbers necessary to choose a single transition. Therefore we rearrange each column in  $P$  by permuting its elements into decreasing magnitude from the top, and obtain a new probability matrix  $P'$  and an integer matrix  $I (P, P')$  to keep in check the correspondence between  $P$  and  $P'$ . This sorting work is done by the subroutine SORT, which also converts  $P'$  to a cumulative distribution matrix  $P''$ .

#### 2.3.3. Direct Simulation Block

Direct simulation is used in the Monte Carlo sampling of the neutron transport in the heterogeneity. Intercollision distances are governed by the macroscopic transport cross-sections in each region. A set of geometrical routines keep track of the position and the momentary region of the particle along its trajectory. These routines of course depend on the actual fine-structure of the heterogeneity. In the present version of MOVAX the geometry is that of fig. 2, but the modular structure of the code makes it quite easy to replace the geometrical routines by some others. Lattice repetitions and symmetries are taken into account as reflection planes. Group transitions after scattering are sampled from the matrix  $P''$  (2.3.2.). Direction cosines after scattering

are picked from an isotropic distribution. When a trajectory is terminated by returning to the boundary, the current and flux contributions  $-1$  and  $\frac{1}{\cos\theta_i}$  are scored in the appropriate group (cf. sec.2.2.).

#### 2.3.4. Estimates of $\underline{A}$ and $\underline{B}$

After completion of one sample block, which contains altogether  $N \times G$  trajectories, all individual score contributions are averaged and combined with the fixed initial contributions ((12) and (13)) to give estimates of the columns of  $\underline{A}$  and  $\underline{B}$  ((16) and (17)).

#### 2.3.5. $\gamma$ -Estimate by Matrix Inversion

At this stage an estimate of  $\underline{Y}$  is computed from

$$\underline{Y} = \underline{A} \underline{B}^{-1} \quad (20)$$

The matrix inversion is accomplished by a linear-equation solver consisting of the two subroutines DECOMP and SOLVE. These routines, which use Gaussian elimination, are written by Moler<sup>3)</sup>.

#### 2.3.6. Statistical Processing

Whereas the number of iterations in the inner loop (fig. 4) is governed by the prescribed value  $N$ , the outer iterations are stopped by a clock in MOVAX, when a prescribed CPU-limit is exceeded. At this time  $K$  different estimates of  $\underline{Y}$  have been computed and stored in an external file, which is now ready to be analysed statistically. This is done by the general subroutine STAT1 which calculates all the sample means for the multi-dimensional sample and estimates the standard deviations of the means.

#### 2.3.7. Output

The lineprinter output contains all input data and the Monte Carlo estimate of the  $\gamma$ -matrix with associated estimates of standard deviations. The program is also able to give the  $\gamma$ -matrix in punched-card form.

### 3. TEST OF THE MOVAX PROGRAM

#### 3.1. Comparisons with other Methods

It has been pointed out earlier that the validity of the  $\gamma$ -matrix method was dependent on the situation of the boundary. It is also obvious that the method used in realizing the G different physical situations may give a rather anisotropic boundary flux for the calculation of the  $\gamma$ -matrix.

Considering the first point, it has been shown in refs. 2, 4 and 5 that a  $\gamma$ -matrix can be used with satisfactory results as boundary condition for a diffusion calculation, both in one dimension for an absorbing slab and in two dimensions for a cruciform control rod in a fuel box.

As for the second point, it should be expected that the effect of the anisotropic flux would be strongest for a strong absorber, while a big selfscattering cross section in the starter group will tend to eliminate the anisotropy of the flux. In order to check this, three calculations have been carried out in the geometry shown in fig. 5.

In the three runs the thickness of the H<sub>2</sub>O slab has been 0 cm (that is, only a B<sub>4</sub>C slab), 1 cm and 4 cm. For the same geometries, collision probability calculations of the  $\gamma$ -matrix have been made by means of HECS<sup>1)</sup>. The results are given in table 1a, 1b and 1c.

Although the  $\gamma$ -matrices calculated by HECS do not eliminate the effect of the anisotropy, this effect should decrease when the selfscatter increases, as it did for the Monte Carlo calculation, and eventually the two methods should give the same results. A comparison between the matrices for case no 3 does show agreement within the estimated statistical uncertainty.

A direct comparison between  $\gamma$ -matrices provides only to some extent a measure of the agreement of the two methods of calculation. In order to give some impression of how much a change in the  $\gamma$ -matrix affects a diffusion calculation, a one-dimensional diffusion calculation for the geometry shown in fig. 6 was set up.

$k_{\text{eff}}$  was calculated using the  $\gamma$ -matrices from case 1, i.e. for the B<sub>4</sub>C slab. We obtain

	$\gamma$ -matrix by HECS	$\gamma$ -matrix by MOVAX
Keff	0.93963	0.93734

This result also indicates that the difference between the two methods of treating the anisotropy at the boundary does not affect the results considerably.

One last remark should be made. Considering the matrices calculated by HECS for cases 2 and 3 it is seen that  $\gamma_{44} > 0.5$ .

This is not in agreement with equations (8) and (9). This result stems from the transformation of boundary conditions from  $J_{in}^g$  and  $J_{out}^g$  to  $J^g$  and  $\phi_s^g$ . When these latter are used, the condition  $J_{in}^g > 0$  and  $J_{out}^g > 0$  need no longer be fulfilled.

It should therefore be emphasized that the  $\gamma$ -matrix is a useful but approximate method to treat heterogeneities.

### 3.2. Test of Statistical Stability

It was pointed out in sec. 2.2. that a study of the statistical stability and quality of the method should involve observed results of diffusion calculations applying  $\gamma$ -matrices from MOVAX, rather than the  $\gamma$ -matrix itself.

A series of 10 combined MOVAX/diffusion calculations was carried out for a BWR fuel box with a control rod (fig. 7). Each calculation comprised  $M=4096$  neutron histories in MOVAX (which took 80 sec. CPU-time on a Burroughs 6700). The input data were identical, apart from the different initial pseudo-random integers. The output  $\gamma$ -matrices from MOVAX were fed into the diffusion program DIFF 2D<sup>6)</sup> which calculated  $k_{eff}$  for the box. Then another series of 10 calculations was performed, but this time  $M=40960$  starters were processed in each run. The results from both series are collected in table 2 together with the sample standard deviations on individual runs.

It is seen that  $S_{4096} \sim \sqrt{10} S_{40960}$  as is to be expected in a statistically stable system. However, a sample size larger than 10 would have been desirable to support this conclusion. Another result that can be extracted from table 2 is that the cost for obtaining a reasonably accurate  $\gamma$ -matrix amounts to

about 40000-50000 Monte Carlo histories. This is equivalent to 15 min. CPU-time on B 6700 or approximately 1 min. on an IBM 370/165. Compared to the total computing time spent on a reactor calculation this is not overwhelming.

#### 4. CONCLUSION

It has been shown how heterogeneities can be treated by means of the  $\gamma$ -matrix concept. This concept has been used successfully at Risø for some time, both for control rods and reflectors.

The calculation of a  $\gamma$ -matrix for a BWR control rod by means of the Monte Carlo code MOVAX has only been checked to some extent. A calculation for an actual reactor has not yet been performed. This should be done, and in that connection the problem of finding a suitable set of few group cross sections for the MOVAX calculations should be investigated. In this respect this report should be considered preliminary.

REFERENCES

- 1) J. Pedersen, Calculation of Heterogeneous Constants for Cylinders and Slabs. Risø-M-850 (1969) 23 pp.
- 2) A.M. Hvidtfeldt Larsen, H. Larsen and T. Petersen, Calculations on a Boiling Water Reactor as a Test of the Risø Reactor Code Complex. Risø Report No. 268 (1972) 102 pp.
- 3) C.B. Moler, Matrix Computations with Fortran and Paging. Com. ACM 15 (1972) 4, 268-270 and 274.
- 4) T. Petersen, Repræsentation af kontrolstave, Master Thesis, (Danish Atomic Energy Commission, Risø, 1970) (In Danish) 99 pp.
- 5) H. Larsen, Risø, Denmark, to be published.
- 6) C.F. Højerup, User's Manual for the Program DIFF2D. Risø-M-1439 (1971) (Internal Report) 9 pp.

$\gamma$ calculated by MOVAX	8.63·10 <sup>-3</sup>	0.	0.	0.	0.	0.
	-6.39·10 <sup>-3</sup>	1.62·10 <sup>-2</sup>	0.	0.	0.	0.
	-7.11·10 <sup>-5</sup>	-2.32·10 <sup>-3</sup>	2.53·10 <sup>-1</sup>	0.	0.	0.
	-1.05·10 <sup>-8</sup>	5.24·10 <sup>-7</sup>	-1.22·10 <sup>-4</sup>	4.91·10 <sup>-1</sup>	0.	0.
	6.88·10 <sup>-12</sup>	-4.57·10 <sup>-10</sup>	8.93·10 <sup>-8</sup>	5.85·10 <sup>-4</sup>	4.97·10 <sup>-1</sup>	0.
$\gamma$ calculated by HECS	8.79·10 <sup>-3</sup>	0.	0.	0.	0.	0.
	-6.57·10 <sup>-3</sup>	1.55·10 <sup>-2</sup>	0.	0.	0.	0.
	-2.58·10 <sup>-5</sup>	-2.18·10 <sup>-3</sup>	2.42·10 <sup>-1</sup>	0.	0.	0.
	-3.84·10 <sup>-9</sup>	-2.75·10 <sup>-7</sup>	-1.28·10 <sup>-4</sup>	4.93·10 <sup>-1</sup>	-1.08·10 <sup>-6</sup>	0.
	-4.44·10 <sup>-11</sup>	-2.34·10 <sup>-10</sup>	-1.10·10 <sup>-7</sup>	-4.19·10 <sup>-4</sup>	4.98·10 <sup>-1</sup>	0.
<u>s</u>	1.97·10 <sup>-4</sup>	0.	0.	0.	0.	0.
	1.73·10 <sup>-4</sup>	2.90·10 <sup>-4</sup>	0.	0.	0.	0.
	4.84·10 <sup>-5</sup>	1.46·10 <sup>-4</sup>	1.28·10 <sup>-3</sup>	0.	0.	0.
	5.59·10 <sup>-9</sup>	2.33·10 <sup>-7</sup>	4.20·10 <sup>-5</sup>	5.02·10 <sup>-4</sup>	0.	0.
	4.89·10 <sup>-12</sup>	2.84·10 <sup>-10</sup>	5.16·10 <sup>-8</sup>	1.06·10 <sup>-4</sup>	3.86·10 <sup>-4</sup>	0.

Table 1 a  
 $\gamma$ -matrices for B<sub>4</sub>C slab.



<p style="text-align: center;"><math>\gamma</math> calculated by MOVAX</p>	8.76·10 <sup>-2</sup>	0.	0.	0.	0.
	-7.80·10 <sup>-2</sup>	1.34·10 <sup>-1</sup>	0.	0.	0.
	-5.66·10 <sup>-3</sup>	-1.01·10 <sup>-1</sup>	2.31·10 <sup>-1</sup>	0.	0.
	-5.77·10 <sup>-5</sup>	-2.17·10 <sup>-3</sup>	-2.76·10 <sup>-2</sup>	4.99·10 <sup>-1</sup>	1.59·10 <sup>-5</sup>
	-2.14·10 <sup>-5</sup>	-2.10·10 <sup>-3</sup>	1.95·10 <sup>-2</sup>	-2.02·10 <sup>-1</sup>	1.61·10 <sup>-1</sup>
<p style="text-align: center;"><math>\gamma</math> calculated by HECS</p>	8.11·10 <sup>-2</sup>	0.	0.	0.	0.
	-6.79·10 <sup>-2</sup>	1.28·10 <sup>-1</sup>	0.	0.	0.
	-7.94·10 <sup>-3</sup>	-9.38·10 <sup>-2</sup>	2.32·10 <sup>-1</sup>	0.	0.
	-2.25·10 <sup>-4</sup>	-2.53·10 <sup>-3</sup>	-2.37·10 <sup>-2</sup>	5.04·10 <sup>-1</sup>	-3.00·10 <sup>-5</sup>
	-2.21·10 <sup>-4</sup>	-2.46·10 <sup>-3</sup>	-2.20·10 <sup>-2</sup>	-2.05·10 <sup>-1</sup>	1.72·10 <sup>-1</sup>
<p style="text-align: center;"><math>\underline{s}</math></p>	7.89·10 <sup>-4</sup>	0.	0.	0.	0.
	1.49·10 <sup>-3</sup>	1.12·10 <sup>-3</sup>	0.	0.	0.
	1.08·10 <sup>-3</sup>	1.51·10 <sup>-3</sup>	1.63·10 <sup>-3</sup>	0.	0.
	1.79·10 <sup>-4</sup>	4.77·10 <sup>-4</sup>	1.26·10 <sup>-3</sup>	1.68·10 <sup>-4</sup>	1.59·10 <sup>-5</sup>
	1.42·10 <sup>-4</sup>	3.39·10 <sup>-4</sup>	7.37·10 <sup>-4</sup>	1.65·10 <sup>-3</sup>	1.30·10 <sup>-3</sup>

Table 1 b  
 $\gamma$ -matrices for B<sub>4</sub>C + 1cm H<sub>2</sub>O slab.

$\gamma$ calculated by MOVAX	$3.15 \cdot 10^{-1}$	0.	0.	0.	0.
	$-1.50 \cdot 10^{-1}$	$3.28 \cdot 10^{-1}$	0.	0.	0.
	$-6.14 \cdot 10^{-2}$	$-1.84 \cdot 10^{-1}$	$2.40 \cdot 10^{-1}$	0.	0.
	$-4.68 \cdot 10^{-3}$	$-7.40 \cdot 10^{-3}$	$-3.67 \cdot 10^{-2}$	$5.00 \cdot 10^{-1}$	$4.64 \cdot 10^{-14}$
	$-2.13 \cdot 10^{-2}$	$-3.80 \cdot 10^{-2}$	$-8.30 \cdot 10^{-2}$	$-3.67 \cdot 10^{-1}$	$6.28 \cdot 10^{-2}$
$\gamma$ calculated by HECS	$2.98 \cdot 10^{-1}$	0.	0.	0.	0.
	$-1.43 \cdot 10^{-1}$	$3.35 \cdot 10^{-1}$	0.	0.	0.
	$-6.01 \cdot 10^{-2}$	$-1.82 \cdot 10^{-1}$	$2.43 \cdot 10^{-1}$	0.	0.
	$-3.88 \cdot 10^{-3}$	$-9.44 \cdot 10^{-3}$	$-3.46 \cdot 10^{-2}$	$5.06 \cdot 10^{-1}$	$-5.43 \cdot 10^{-5}$
	$-2.03 \cdot 10^{-2}$	$-3.98 \cdot 10^{-2}$	$-8.71 \cdot 10^{-2}$	$-3.74 \cdot 10^{-1}$	$6.28 \cdot 10^{-2}$
$\underline{s}$	$2.18 \cdot 10^{-3}$	0.	0.	0.	0.
	$2.94 \cdot 10^{-3}$	$2.66 \cdot 10^{-3}$	0.	0.	0.
	$2.22 \cdot 10^{-3}$	$3.16 \cdot 10^{-3}$	$2.94 \cdot 10^{-3}$	0.	0.
	$1.02 \cdot 10^{-3}$	$1.54 \cdot 10^{-3}$	$2.03 \cdot 10^{-3}$	$7.44 \cdot 10^{-5}$	$4.64 \cdot 10^{-14}$
	$1.25 \cdot 10^{-3}$	$1.97 \cdot 10^{-3}$	$2.25 \cdot 10^{-3}$	$3.06 \cdot 10^{-3}$	$1.49 \cdot 10^{-3}$

Table 1 c  
 $\gamma$ -matrices for B<sub>4</sub>C + 4 cm H<sub>2</sub>O slab.

No of neutron histories M = 4096		No of neutron histories M = 40960	
Calc. no.	Keff	Calc. no.	Keff
1	1.1541	1	1.1539
2	1.1557	2	1.1534
3	1.1531	3	1.1540
4	1.1553	4	1.1545
5	1.1537	5	1.1538
6	1.1539	6	1.1535
7	1.1548	7	1.1535
8	1.1545	8	1.1536
9	1.1521	9	1.1535
10	1.1549	10	1.1536
avg. 1.1542 s.d. 0.0010		avg. 1.1537 s.d. 0.00032	

Table 2  
Test of statistical stability of MOVAX.

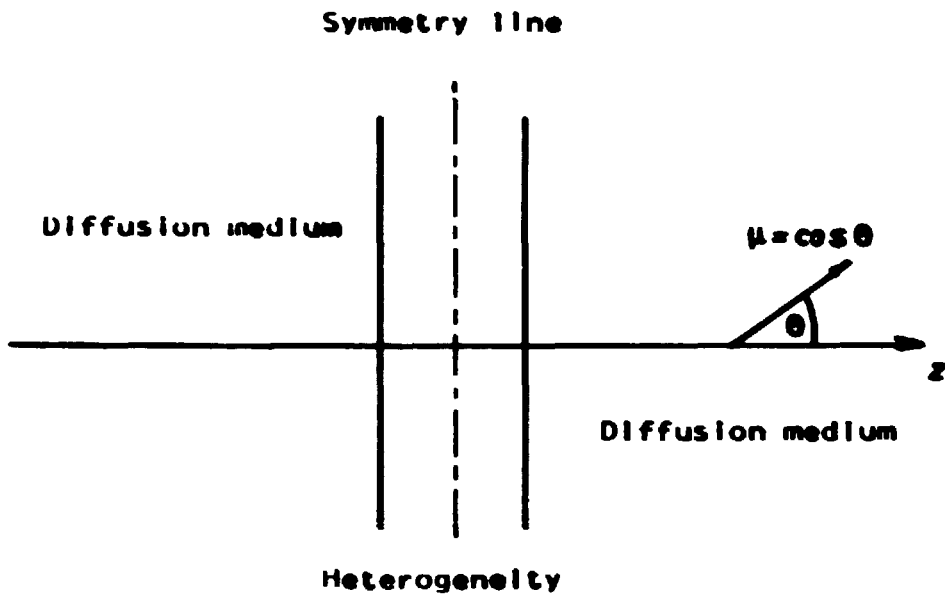


**Fig.1** Symmetrical heterogeneity  
in slab geometry.

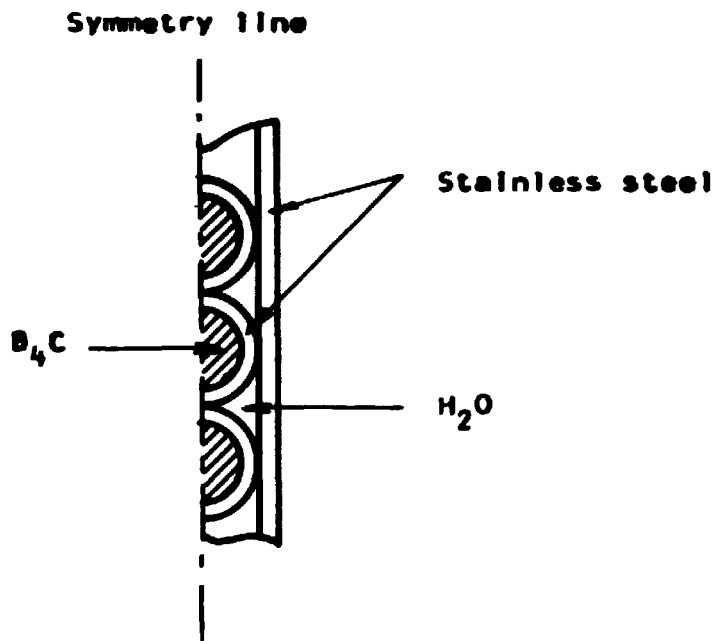


**Fig.2** Typical structure of control rod blade  
in a cruciform control rod for a BWR.

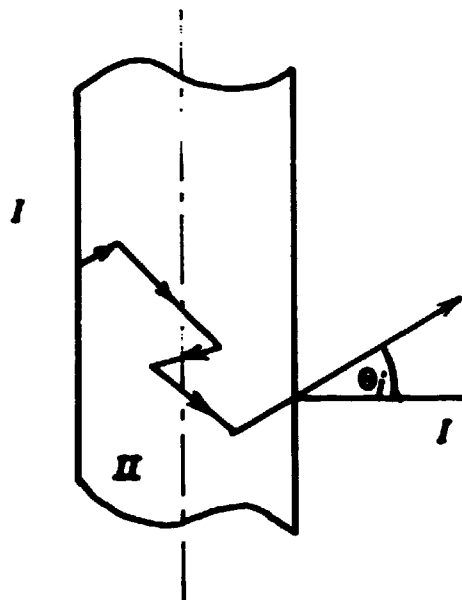


**Fig.3** Trajectory in Monte Carlo treatment of heterogeneity.

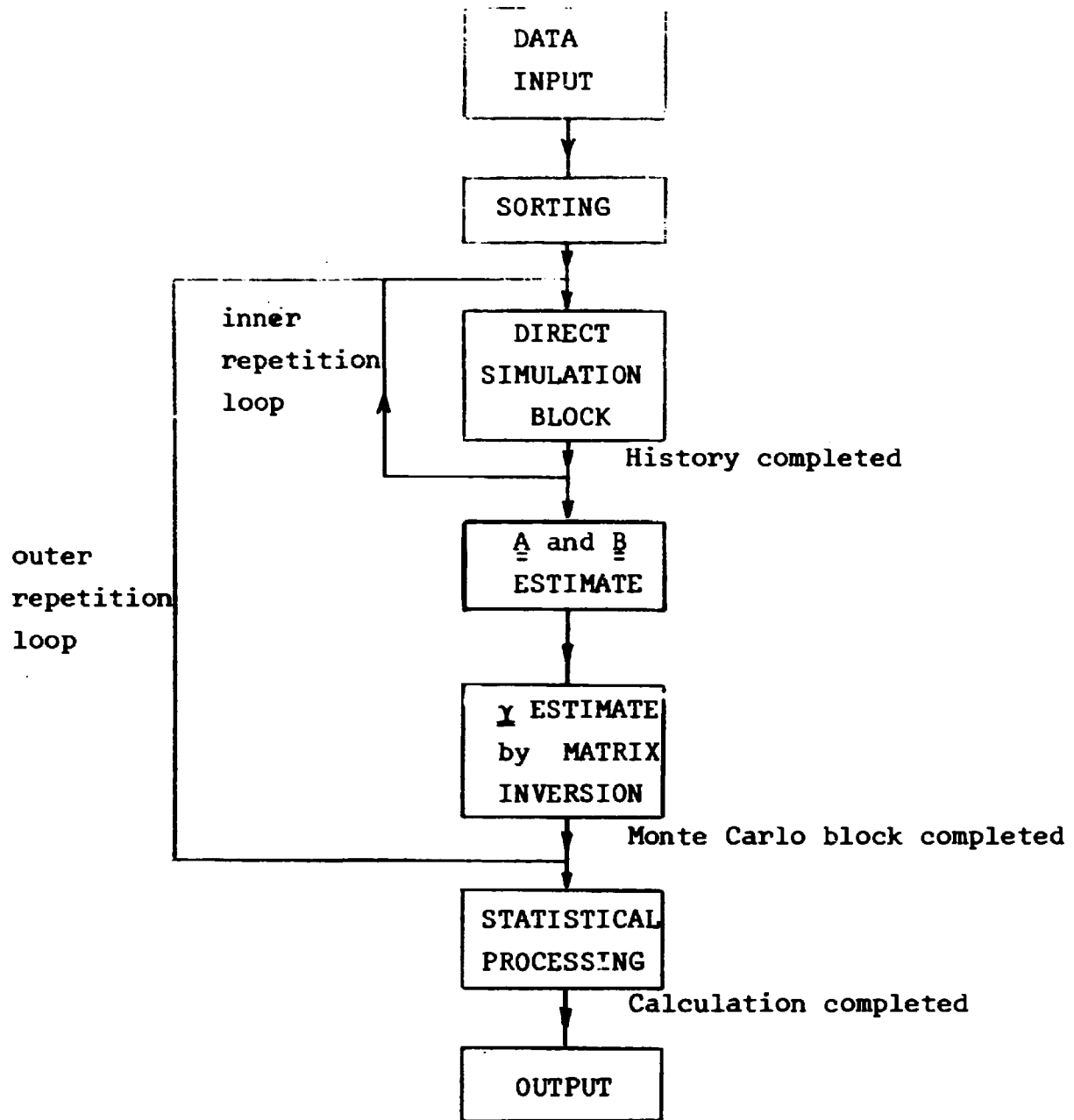
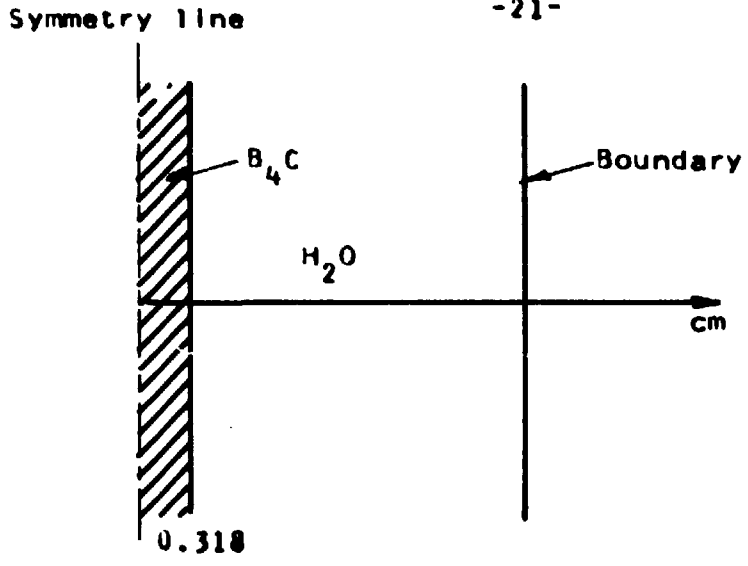
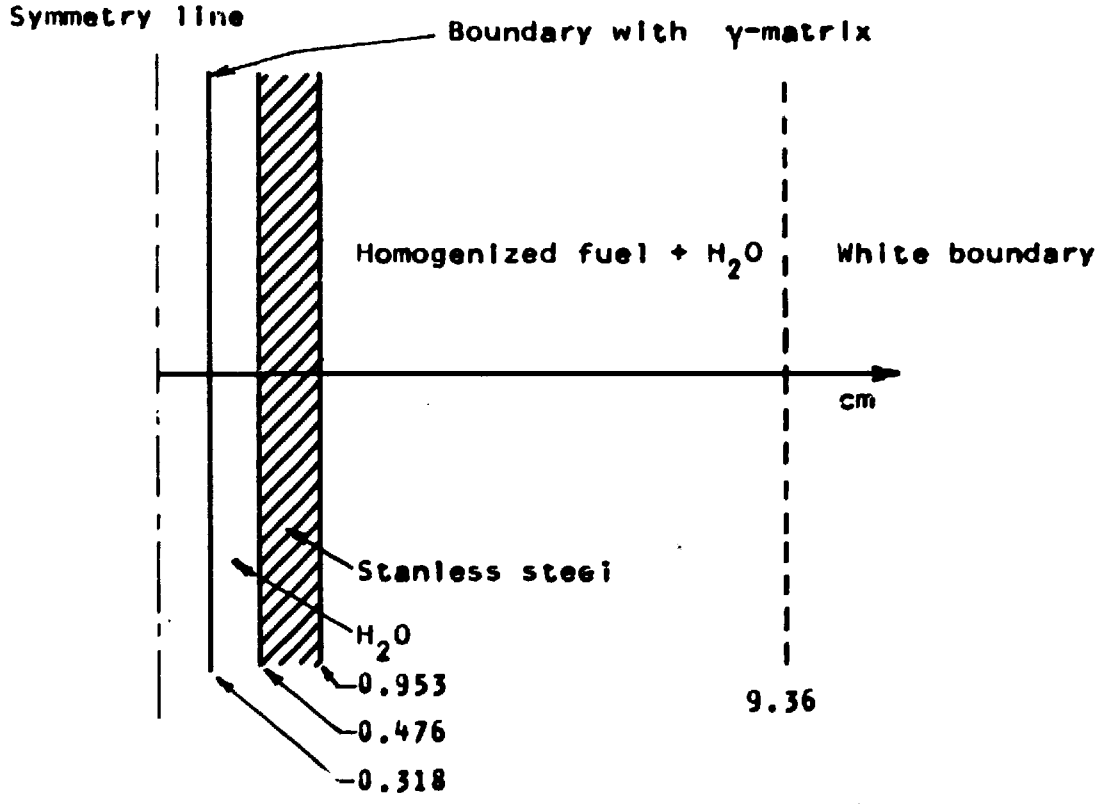


Fig. 4. Flow diagram for Monte Carlo code MOVAX



**Fig.5** Slab used for illustration of the influence of anisotropic boundary flux on the  $\gamma$ -matrix



**Fig.6** Geometry for comparative calculation with  $\gamma$ -matrices.

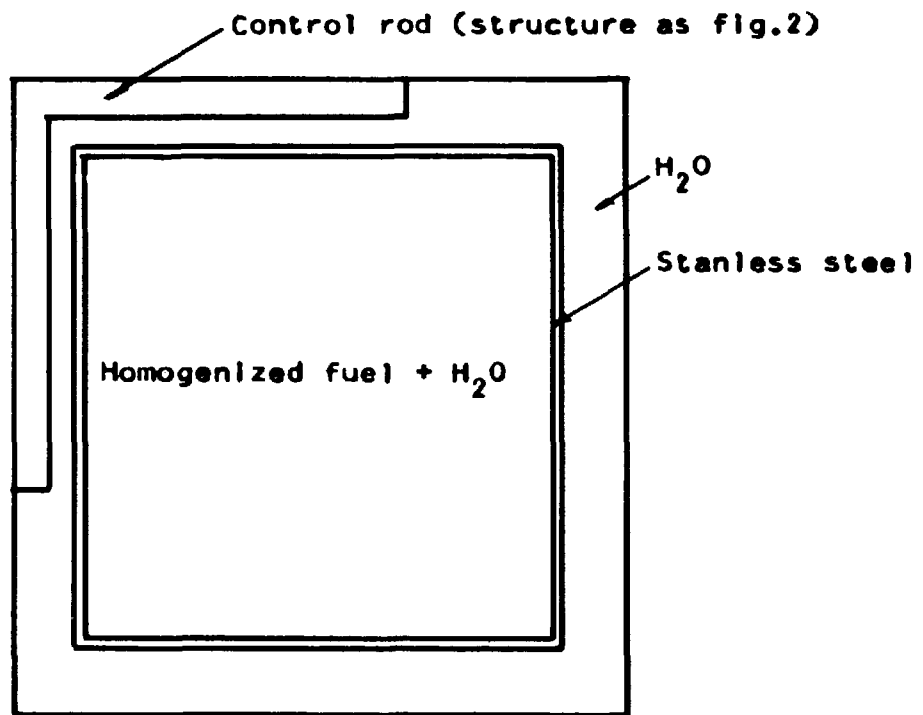


**Fig.7** Typical BWR fuel box used for test of statistical stability of MOVAX